

See discussions, stats, and author profiles for this publication at: <https://www.researchgate.net/publication/270097359>

# Binding of 2-Azaanthraquinone Derivatives to DNA and Their Interference with the Activity of DNA Topoisomerases in Vitro†

ARTICLE · JANUARY 1998

---

READS

11

9 AUTHORS, INCLUDING:

[Andreas Opitz](#)

10 PUBLICATIONS 87 CITATIONS

SEE PROFILE

# Binding of 2-Azaanthraquinone Derivatives to DNA and Their Interference with the Activity of DNA Topoisomerases in Vitro<sup>†</sup>

Günther Burckhardt, Axel Walter, Hans Triebel, Karin Störl, Hannelore Simon, Joachim Störl, Andreas Opitz, Ernst Roemer,<sup>‡</sup> and Christoph Zimmer\*

Departments of Molecular Biology and Biophysical Chemistry, Institute of Molecular Biology, Friedrich Schiller University Jena, Winzerlaer Strasse 10, D-07745 Jena, Germany, and Department of Chemistry, Hans Knöll Institute for Natural Products Research, Beutenberg Strasse 11, D-07745 Jena, Germany

Received September 30, 1997; Revised Manuscript Received January 21, 1998

**ABSTRACT:** We have investigated the binding ability to DNA of compounds belonging to the 2-azaanthraquinone-type structure and have examined the effect on the activity of DNA gyrase as well as on mammalian topoisomerases in vitro. Using different biophysical techniques it was found that one of these ligands, 9-((2-dimethylamino)ethyl)amino-6-hydroxy-7-methoxy-5,10-dihydroxybenzo[g]isoquinoline-5,10-dione (TPL-I), is an intercalating DNA binding agent, whereas the parent compound tolypocladin (TPL) and a derivative (TPL-II) showed almost no similar affinity to DNA. CD measurements demonstrated a significant and selective binding tendency of TPL-I to alternating purine/pyrimidine sequences with some preference for poly(dA-dT)·poly(dA-dT). *T<sub>m</sub>* values were increased of the ligand complex with the alternating AT-containing duplex polymer. The binding to various DNAs was characterized by CD and visible absorption spectral changes. From the latter, different binding constants of  $6.2 \times 10^5$  and  $1.5 \times 10^5 \text{ M}^{-1}$  were obtained for poly(dA-dT)·poly(dA-dT) and poly(dA)·poly(dT), respectively. Sedimentation measurements with supercoiled pBR322 plasmid DNA clearly indicated an intercalative binding mechanism associated with an unwinding angle of about 18°. These results suggest that the intercalative binding of TPL-I is promoted by the 2-(dimethylamino)ethylamino group substituted on carbon 9 of the anthraquinone system. The cytotoxic compound TPL-I, but not TPL or TPL-II, effectively inhibited the DNA supercoiling reaction of DNA gyrase and the activity of mammalian topoisomerases I and II as measured by the relaxation assay. TPL-I affects the cleavage reaction of topoisomerases on a single site located in alternating purine–pyrimidine sequence regions. The inhibitory potency of TPL-I can be ascribed to a blocking of cleavage sites on the DNA substrate, which correlates with the sequence preference of the ligand.

Tolypocladin, a pigmented metabolite derived from the mycelium of *Tolypocladium inflatum* (1) was identified as 6,7,9-trihydroxy-3-methyl-5,10-dihydrobenzo[g]isoquinoline-5,10-dione.

The biological role of this metabolite is not yet known. Tolypocladin and some derivatives show cytotoxic activity (Gutsche, unpublished). At first glance the chromophore of this class of compounds seems to possess structural similarities to the group of anthracene-9,10-diones, such as mitoxantrone (2–4), but it differs markedly with respect to the location of the ring nitrogen and various side chain substitutions (Figure 1). More recently, a new type of modified antitumor anthracene-9,10-diones was reported (5). Whereas an intercalative interaction mechanism of mitoxantrone with DNA has been widely demonstrated (3, 4, 6, 7), studies with

2-azaanthraquinones have not been reported so far. Topoisomerases are potential drug targets and a number of antitumor active compounds or antibiotics inhibit the enzymic activity by interference with the DNA–enzyme complex (8–12). Many inhibitors interact with the enzyme, such as the anti-gyrase active compounds quinolones or coumarins (8, 11). The drug camptothecin binds to the DNA–topoisomerase I complex, but not to the isolated DNA or enzyme protein (9). On the other hand, mitoxantrone as a DNA binding agent may also stimulate mammalian topoisomerase II cleavage activity in vitro (13).

In this work we investigated the binding ability to DNA of tolypocladin (TPL) and two synthetic analogues and compared their inhibitory effects on the activity of DNA topoisomerases in vitro. As evidenced from several biophysical experiments a TPL analogue (TPL-I, cf. Figure 1) shows a profound affinity to DNA whereas the parent compound TPL is inactive. TPL-I binds to DNA by means of intercalation and inhibits DNA gyrase as well as mammalian type I and II topoisomerases in vitro.

<sup>†</sup> This work was supported in part by Deutsche Forschungsgemeinschaft (Grant Zi 396/5-1) and Thüringer Ministerium für Wissenschaft, Forschung U. Kuetur.

\* To whom correspondence should be addressed. Tel.: +49 3641 65 7500. Fax: +49 3641 65 7520. E-mail: christoph.zimmer@uni-jena.de.

<sup>‡</sup> Hans Knöll Institute for Natural Products Research.

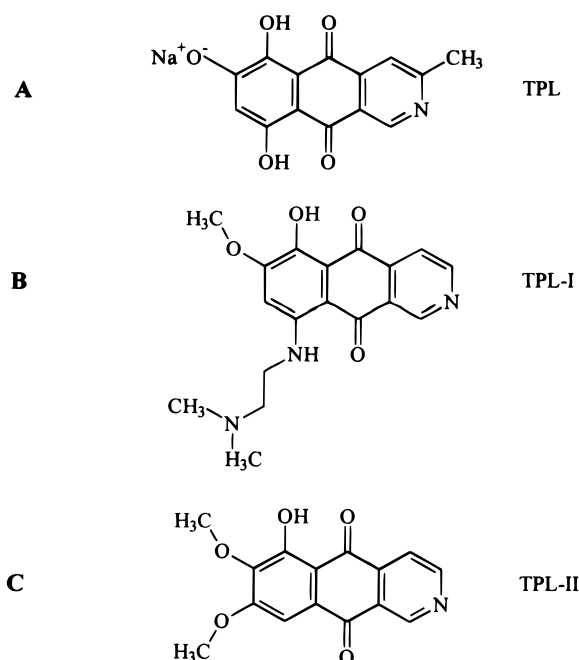


FIGURE 1: Chemical structures of 2-azaanthraquinone derivatives. (A) Tolypocladin, sodium salt (TPL). (B) Tolypocladin analog-I (TPL-I). (C) Tolypocladin analog-II (TPL-II).

## EXPERIMENTAL PROCEDURES

**Materials.** DNA samples from calf thymus (CT DNA: 58 mol % AT) and GC-rich DNA from *Streptomyces chrysomallus* (SC DNA: 28 mol % AT) were purified and used as previously described (14). Synthetic DNA duplex polymers were from Boehringer (Mannheim) and used without further purification. Molar extinction coefficients in base pair (bp) units (for 1 cm path length) were used as follows: poly(dA)•poly(dT),  $\epsilon_{260} = 12.0 \text{ mM}^{-1} \text{ cm}^{-1}$ ; poly(dA-dT)•poly(dA-dT),  $\epsilon_{262} = 13.6 \text{ mM}^{-1} \text{ cm}^{-1}$ ; poly(dG-dC)•poly(dG-dC),  $\epsilon_{254} = 14.2 \text{ mM}^{-1} \text{ cm}^{-1}$ ; poly(dA-dC)•poly(dG-dT),  $\epsilon_{260} = 13.0 \text{ mM}^{-1} \text{ cm}^{-1}$ . Supercoiled plasmid DNA from pBR322 was isolated according to standard procedures by CsCl density gradient centrifugation or was purchased from Sigma; the molar absorption coefficient used was  $\epsilon_{260} = 6.62 \times 10^3 \text{ M}^{-1} \text{ cm}^{-1}$ ; samples differed somewhat in their superhelix density. Plasmid pUCNC15 was a generous gift from O. Westergaard (Åarhus, Denmark; cf. ref 15). Tolypocladin (TPL) and two synthetic congeners (TPL-I and TPL-II, cf. Figure 1) were obtained from the Hans Knöll Institute; extinction coefficients used are TPL,  $\epsilon_{526} = 6.2 \times 10^3 \text{ M}^{-1} \text{ cm}^{-1}$ ; TPL-I,  $\epsilon_{563} = 7.63 \times 10^3 \text{ M}^{-1} \text{ cm}^{-1}$ ; and TPL-II,  $\epsilon_{285} = 2.01 \times 10^3 \text{ M}^{-1} \text{ cm}^{-1}$ .

Restriction enzymes were purchased from Bio Labs; Klenow enzyme was from Boehringer Mannheim; [ $^{32}\text{P}$ ]-dATP was from NEN; and camptothecin was from Sigma. Kinetoplast DNA (kDNA) was prepared from *Crithidia fasciculata* according to Hajduk et al. (16).

DNA gyrase from *Streptomyces noursei* was purified to homogeneity as reported elsewhere (17). Briefly, a crude extract obtained from a continuous culture of *S. noursei* N840 was applied for purification on a novobiocin-Sepharose column; the native enzyme A2B2 was eluted with 20 mM ATP. Eukaryotic topoisomerases I and II were isolated simultaneously as described by Strausfeld and Richter (18).

Topoisomerase I was identified by relaxation of supercoiled pBR322 DNA in the absence of ATP. Topoisomerase II was assayed by decatenation of kDNA in the presence of ATP (19). The purified enzymes were devoid of cross-contamination. They were dialyzed against storage buffer (20 mM Tris-HCl, pH 7.5, 1 mM EDTA, 10 mM  $\text{Na}_2\text{S}_2\text{O}_5$ , 10 mM 2-mercaptoethanol, 0.2 M NaCl, 50% glycerol) and stored at  $-20^\circ\text{C}$ . The specific activities of the enzymes were approximately  $5 \times 10^6$  units/mg of protein. One enzyme unit is defined as the activity fully relaxing  $0.5 \mu\text{g}$  of pBR322 DNA at  $37^\circ\text{C}$  in 30 min in a standard assay.

**DNA Fragments.** The 162 bp restriction fragment from pBR322 was obtained as previously reported (20); the 249 bp *EcoRI*–*PvuII* fragment containing a high-affinity site for topoisomerase I (15) was isolated from the plasmid pUC-NC15; it was labeled at the recessed 3'-end of the *EcoRI* site using  $\alpha$ -[ $^{32}\text{P}$ ]dATP (3000 Ci/mmol) and the Klenow fragment of DNA polymerase I according to standard procedures.

## Enzyme Assays

Supercoiling reaction of DNA gyrase was described elsewhere (17, 20, 21). The gyrase-mediated cleavage of the 162 bp fragment from pBR322 DNA was performed in the presence of 100 mM ciprofloxacin (Bayer AG, Leverkusen) using an assay described previously (20).

Relaxation standard assay with mammalian topoisomerase I and II has been done using 1 unit of enzyme in  $20 \mu\text{L}$  reaction mixtures containing  $0.6 \mu\text{g}$  of supercoiled pBR322 DNA in 20 mM Tris-HCl, pH 7.8, 150 mM KCl, 10 mM  $\text{MgCl}_2$ , 1 mM EDTA, 1 mM DTT, 200  $\mu\text{g}/\text{mL}$  bovine serum albumin, and, for topoisomerase II, 1 mM ATP. Compounds to be tested were diluted in DMSO<sup>1</sup> to a final DMSO concentration of 10% in the relaxation assay. This amount of DMSO does not influence the enzyme activity. The indicated amounts of inhibitors were preincubated with supercoiled DNA for 10 min at  $37^\circ\text{C}$ . The enzyme reactions were terminated by addition of  $5 \mu\text{L}$  of stopper solution containing 0.5% sodium dodecyl sulfate, 1 mg/mL proteinase K, and 1 mM  $\text{CaCl}_2$  in 50 mM Tris-HCl, pH 7.8, and incubation at  $50^\circ\text{C}$  for 15 min. After addition of  $5 \mu\text{L}$  of 0.005% bromophenol blue in 50% glycerol, the samples were analyzed on 1% agarose gels in TAE buffer (50 mM Tris-acetate, pH 8.0, 20 mM sodium acetate, 2 mM EDTA, 18 mM NaCl). Electrophoresis was carried out at 2 V/cm overnight. The gels were stained with ethidium bromide and photographed under UV illumination. Inhibitory effects are given as  $\text{IC}_{50}$  and  $\text{IC}_{90}$ , representing those concentrations of substances which cause medium or nearly complete inhibition of enzyme reactions, respectively.

The topoisomerase-mediated DNA cleavage was performed in reaction mixtures of  $48 \mu\text{L}$  containing  $5 \mu\text{L}$  of reaction buffer (500 mM Tris-HCl, pH 7.6, 250 mM KCl, 10 mM DTT),  $2 \mu\text{L}$  of labeled fragment (30 000–50 000 cpm; 5–12 ng),  $1 \mu\text{L}$  of camptothecin solution (10 mM in DMSO),  $5 \mu\text{L}$  of inhibitor, resulting in the final concentration as indicated,  $2 \mu\text{L}$  of glycerol, and  $33 \mu\text{L}$  of  $\text{H}_2\text{O}$ . Reactions were initiated by the addition of  $2 \mu\text{L}$  of topoisomerase I

<sup>1</sup> Abbreviations: DMSO, dimethyl sulfoxide; DTT, dithiothreitol; VM 26, teniposide [4'-demethylepipodophyllotoxin thenylidene  $\beta'$ -D-glucoside].

(80 units). Reaction mixtures were incubated for 30 min at 30 °C, and the reactions were stopped with 200  $\mu$ L of 0.5% SDS followed by 5  $\mu$ L of proteinase K (20 mg/mL) and incubation at 55 °C for 1 h.

After addition of 1  $\mu$ L of tRNA (10 mg/mL), the samples were deproteinized with phenol/chloroform, precipitated with ethanol and resuspended in 4  $\mu$ L of 80% formamide, 10 mM NaOH, 1 mM EDTA, 0.1% bromophenol blue, and 0.1% xylene cyanole FF. After heating for 10 min the samples (30,000 cpm/lane) were resolved by electrophoresis in 8 M urea, 8% polyacrylamide sequencing gels in 100 mM Tris-borate, pH 8.3, and 2 mM EDTA. The cleavage products were compared with sequencing ladders generated by the Maxam–Gilbert method. Reaction products were visualized by autoradiography or a Phosphor Imager system.

Reaction buffer (10 $\times$ ) for the topoisomerase II-mediated DNA cleavage was 500 mM Tris-HCl, pH 7.6, 250 mM KCl, 10 mM DTT, 10 mM ATP, 60 mM MgCl<sub>2</sub>, and 1  $\mu$ L of VM 26 (3.4 mg/mL DMSO) was added instead of camptothecin.

**Biophysical Binding Experiments.** CD spectra were recorded on a Jasco 720 CD dichrograph using a 1 cm path length cell. Sedimentation velocity experiments were carried out as reported previously (22) using a Beckman model Spinco E analytical ultracentrifuge coupled with an AT 386 personal computer for online data acquisition (23). Absorption spectra were recorded on a Perkin-Elmer Lambda 19 spectrophotometer equipped with thermostated cell holders. In the titration experiments, the extinction at fixed wavelengths was measured with sampling times of at least 10 s. For quantitative binding studies, at least three solutions of different DNA concentration were prepared gravimetrically from a DNA stock solution. These solutions were titrated by adding microliter quantities of a TPL-I stock solution, arriving at final total TPL-I concentrations of approximately 20  $\mu$ M. Besides the actual titration of DNA with the ligand, the concentration dependence of the spectral properties of TPL-I was studied in an analogous way to determine the parameters of self-association. The procedures used in spectrophotometric binding studies, binding modeling, and data handling are described elsewhere (24). Sedimentation and absorption measurements were made in the presence of 50 mM Tris-HCl, 1.0 mM EDTA, pH 7.8 at 20 °C.

**Filter Binding Assay.** Nitrocellulose filters (Schleicher & Schüll, NC 45, 25 mm diameter) were wet soaked in 0.4 M KOH for 30 min at room temperature, rinsed with water to neutrality, and stored in binding buffer (10 mM Tris-HCl, pH 7.6, 60 mM KCl, 10 mM MgCl<sub>2</sub>, 0.1 mM spermidine, 0.1 mM EDTA) at 4 °C. Reaction mixtures (110  $\mu$ L) containing [<sup>32</sup>P]-5'-end-labeled NC14 DNA fragment, topoisomerase I or II (producing 80% of the maximum obtainable filter binding), and the indicated amounts of the ligand were incubated for 30 min at room temperature. Mixtures were then spotted onto prewashed filters using a 10-well filtration apparatus from Hoefer. After the filters were washed under reduced pressure (1–2 mL/min) two times with 500  $\mu$ L of binding buffer containing 25  $\mu$ g/mL of bovine serum albumin, they were dried and counted in a Beckman LS 6000 counter.

**Gel Retardation Assay.** Reaction mixtures with topoisomerases I and II were prepared as for the filter assay. After addition of bromophenol blue in glycerine (as dye

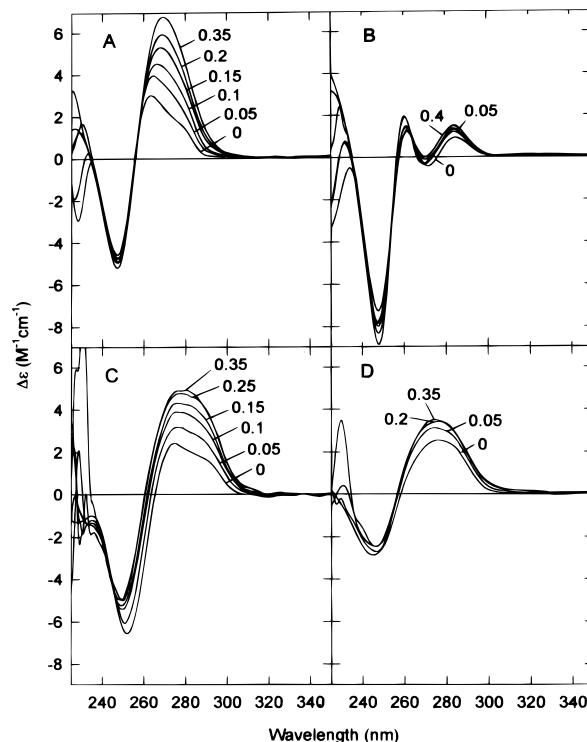


FIGURE 2: CD spectra of TPL-I DNA complexes at 0.1 M NaCl, pH 7. (A) Poly(dA-dT)·poly(dA-dT); (B) poly(dA)·poly(dT); (C) poly(dG-dC)·poly(dG-dC); (D) CT DNA. Attached numbers designate total ratio  $r_t$ , ligand per nucleotide.

marker), the mixtures were loaded into a 5% polyacrylamide gel (90 mM Tris-borate, pH 7.6, 2.5 mM EDTA). Gels were run for 3 h at 0.8 V/cm, dried, and exposed on X-ray film overnight.

## RESULTS

**CD Binding Studies.** Circular dichroism can be used to monitor DNA binding of small organic ligands, in particular when they are optically inactive (25). Figure 2 shows typical CD spectra of various DNA complexes formed with TPL-I. Poly(dA-dT)·poly(dA-dT) and poly(dG-dC)·poly(dG-dC) exhibit a significant enhancement of the positive CD band around 275 nm in the presence of increasing TPL-I concentration, the effect of which is more pronounced for the AT-containing duplex polymer (Figure 2A and C). Because TPL-I is optically inactive, these CD changes directly reflect ligand binding to the duplex structures. Strikingly different behavior is observed for poly(dA)·poly(dT), which does not show a similar large CD binding effect in the presence of increasing amounts of TPL-I under comparable conditions (Figure 2B). The CD titration curves measured at the CD maxima of DNA complexes more clearly demonstrate the variation of the binding ability of TPL-I to different DNA's. As shown in Figure 3, the CD signal progressively increases for the alternating AT- and GC-containing DNA duplex polymers and reaches a saturation level at room temperature of 0.3–0.4, which is the total ratio of TPL-I to nucleotide (Figure 3, curves 1 and 2). In contrast to that for poly(dA)·poly(dT) a titration curve with very low CD signals is observed (Figure 3, curve 6), suggesting a weak affinity of TPL-I to this sequence. The other DNA's exhibit a CD binding behavior with somewhat higher affinity when compared to poly(dA)·poly(dT), but all of them show distinct

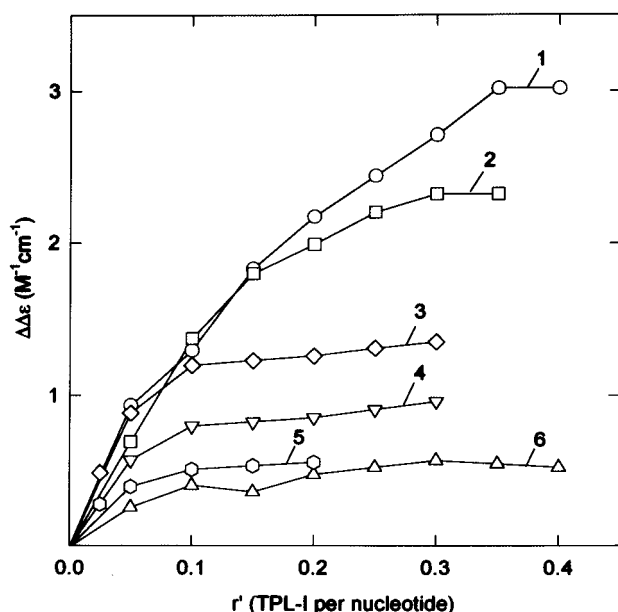


FIGURE 3: CD titration curves of different DNAs with TPL-I in 0.1 M NaCl, monitored at their CD maxima for corresponding curves as indicated: (1) poly(dA-dT)·poly(dA-dT) at 264 nm; (2) poly(dG-dC)·poly(dG-dC) at 274 nm; (3) poly(dA-dC)·poly(dG-dT) at 271 nm; (4) CT DNA at 276 nm; (5) SC DNA at 270 nm; (6) poly(dA)·poly(dT) at 255 nm.

lower affinity relative to the alternating DNA duplex. No similar DNA binding ability was found for TPL or TPL-II in their CD spectra (data not shown). To characterize the stability of the most efficient complex formation of TPL-I with poly(dA-dT)·poly(dA-dT) the influence of increasing salt concentration was investigated. The CD binding effect measured at room temperature is 0.4 (total ratio of TPL-I per nucleotide), is progressively lowered from  $\Delta\epsilon = 6 \text{ M}^{-1} \text{ cm}^{-1}$  at 0.1 M NaCl (room temperature) to  $\Delta\epsilon = 4.2 \text{ M}^{-1} \text{ cm}^{-1}$  at 1 M NaCl, and becomes totally abolished at 2–4 M NaCl, suggesting complete dissociation of the complex at high salt molarity (data not shown).

#### Melting Temperature and Visible Absorbance Measurements

For DNA–TPL-I complexes at 50 mM NaCl, significant melting temperature changes ( $\Delta T_m$ ) were detected (Table 1). The largest stabilization in temperature occurs for the complex of poly(dA-dT)·poly(dA-dT), which is most pronounced compared to the other DNA complexes studied at the same total ratios of TPL-I to nucleotide.

For further quantitative characterization of TPL-I binding, the difference spectra between DNA–TPL-I complexes and pure ligand were measured. From these spectra which exhibited an isosbestic point near 612 nm (results not shown), indicating a single complex type, we selected those wavelengths at which the absorbance shows the most sensitive response to the binding of TPL-I to DNA. For this purpose the visible spectral range was chosen since within this region only the free and bound ligand and not the DNA contribute to the measured absorbance. For DNA–TPL-I complexes, wavelengths of 520, 560, 600, 630, and 750 nm were selected. The latter one, located beyond the absorption band, indicates light scattering if aggregates or impurities arise during the titration procedure.

In Figure 4 the absorbances measured at the four wavelengths selected are given for the CT DNA–TPL-I complex. With increasing total ligand concentration, a progressive splitting of the titration curves obtained at three different DNA concentrations (which are in the ratio of approximately 1:2:5) can be observed. The curve splitting indicates that a proper DNA concentration range can be selected in our binding experiments. The smooth curve in Figure 5 results from a nonlinear regression analysis including all absorbance values measured at the four wavelengths and the three DNA concentrations. For the calculation of thermodynamic parameters, binding by a single mechanism was assumed and the model of cooperative binding to a homogeneous chain of monomeric units with overlapping binding sites (26, 27) was chosen. Both the binding parameters and the molar extinction coefficients with their errors can be determined by this fitting procedure. Like other planar intercalating drugs, TPL-I shows a strong self-association under our solvent conditions (results not shown). A dimer model of self-association was found to be sufficient to correct the free monomeric ligand concentrations.

In Table 1 are given the binding constant  $K_a$  (for singly contiguous binding), the cooperativity parameter  $\sigma$  ( $\sigma = 1$ , noncooperative binding;  $\sigma < 1$ , cooperative binding), and the size of a binding site  $\beta$  (given in base pairs per bound ligand) for the complexes of TPL-I with polynucleotides and CT DNA. These data show that the strongest binding of TPL-I was found for the alternating polynucleotides poly(dA-dT)·poly(dA-dT) and poly(dG-dC)·poly(dG-dC), a weaker binding for poly(dA-dC)·poly(dG-dT) and CT DNA. The homopolymer poly(dA)·poly(dT) binds approximately by a factor of 4 more weakly compared with the alternating polynucleotides (Table 1). This result is in agreement with the magnitude of the TPL-I-induced Cotton effect in the CD spectral data (see Figures 2 and 3). A distinct GC dependence of the binding strength does not exist. As indicated by the  $\sigma$  values (Table 1), the binding process seems to be slightly cooperative, meaning that the binding of additional TPL-I molecules to DNA is favored by the TPL-I molecules which are already bound. As a consequence of the large errors estimated, however, the significance of these  $\sigma$  values is low. The size of a binding site,  $\beta$ , with a value of approximately 2 base pairs per bound TPL-I, corresponds well to the nearest neighbor exclusion model characteristic of intercalating drugs.

**Analytical Ultracentrifugation.** The aim of boundary sedimentation experiments on supercoiled DNA–drug complexes was to obtain information about the mode of DNA–drug interaction. Figures 6A–C show the sedimentation coefficient of the supercoiled form of pBR322 DNA as a function of increasing drug to nucleotide input ratio for TPL-I, TPL-II, and TPL, respectively. The observation that the sedimentation coefficients of DNA at zero drug concentration differ slightly from each other (Figures 6A–C) is due to the fact that different pBR322 preparations were used within the course of this study (cf. Experimental Procedures). It is obvious that TPL-I has a strong effect on the sedimentation behavior of covalently closed pBR322 DNA. When increasing amounts of TPL-I are added, the sedimentation coefficient of the plasmid DNA undergoes the typical fall and rise (Figure 6A, curve 2), which is known as a characteristic feature of an intercalation process (28). Progressive un-

Table 1: Melting Temperature Data and Binding Parameters of TPL-I Complexes Formed with Various DNAs

	$\Delta T_m^a$ (°C)		$10^{-5} \times K_a^b$ (M <sup>-1</sup> )	$\sigma^b$	$\beta^b$ (bp/TPL-I)
	$r_t = 0.1$	$r_t = 0.2$			
poly(dA)·poly(dT)	2.3	—	(1.5 ± 0.4)	0.57 ± 0.20	2
poly(dA-dT)·poly(dA-dT)	5.7	10.2	(6.2 ± 0.6)	0.26 ± 0.05	1.95 ± 0.08
poly(dG-dC)·poly(dG-dC)	—	—	(5.8 ± 1.3)	0.51 ± 0.21	1.88 ± 0.18
poly(dA-dC)·poly(dG-dT)	2.4	—	(4.0 ± 2.0)	1.27 ± 0.83	1.64 ± 0.28
CT DNA	1.4	2.2	(3.3 ± 1.0)	0.40 ± 0.20	2.07 ± 0.29

<sup>a</sup> Measured in 50 mM NaCl, pH 7, at given  $r_t$ , total ligand per nucleotide. <sup>b</sup> Measured in 50 mM Tris buffer solution, 1 mM EDTA, pH 7.8, at 20 °C.

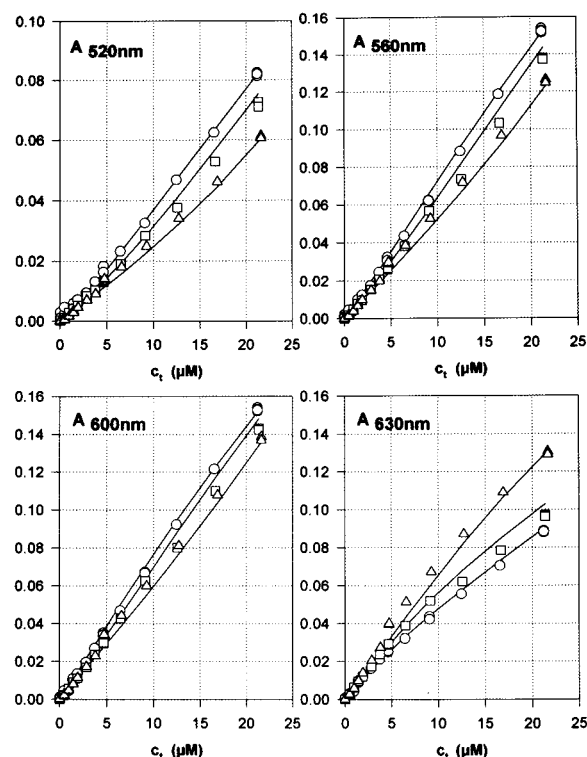


FIGURE 4: Titration curves of CT DNA with TPL-I. Absorbance is plotted as a function of increasing total concentration,  $c_t$ , of the ligand at the selected wavelengths of 520, 560, 600, and 630 nm. Titrations were made at three initial DNA concentrations: (○) 10.4  $\mu$ M; (□) 21.3  $\mu$ M; and (△) 51.3  $\mu$ M in base pairs.

winding of the supercoiled DNA duplex is accompanied by removal and subsequent reversal of supercoils, which on its part produces the response in  $s_{20}$  seen in Figure 6A. The curve minimum represents a kind of titration end point at which the accumulated drug-induced unwinding of the DNA duplex just compensates the initial linking number deficit,  $\Delta Lk$ , of the supercoiled DNA, and, therefore, corresponds to a supercoil-free state of DNA. In comparison with the effect of the classical intercalating drug ethidium (used here as a reference) on the sedimentation coefficient of the same DNA (Figure 6A, curve 1), curve 2 is shifted to higher drug to nucleotide input ratios and exhibits a more asymmetric shape. The experimental data in the vicinity of the curve minima were fitted by third-order polynomials to take this asymmetry into account. The corresponding third-order equations were differentiated, and the derivatives were set equal to zero in order to obtain, by solving the resulting quadratic equations, the coordinates of the curve minima. By this procedure we arrived at the critical drug to nucleo-

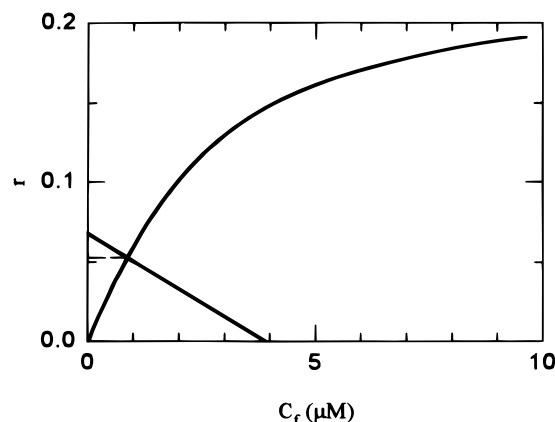


FIGURE 5: Binding isotherm for the complex of CT DNA formed with TPL-I, calculated with the thermodynamic parameters from Table 1. The straight line represents the linear eq 1 (which describes the balance of the total drug concentration) for the experimental conditions existing at the minimum of curve 2 in Figure 6A (cf. eq 1 and text).

tide input ratios,  $(r_c)_t$ , for EB and TPL-I presented in Table 2.

For further quantitative conclusions it is necessary to convert the critical drug to nucleotide input ratios at the curve minima into true drug to nucleotide binding ratios. Since at the critical input ratio,  $(r_c)_t$ , the binding affinity to supercoiled DNA is equal to that of open circular (or linear) DNA (29) and the binding of TPL-I to natural DNA shows no distinct dependence on DNA base composition, at least in the range of medium GC content (Table 1), the binding data obtained on linear CT DNA (Figure 5) may be used as a good approximation to calculate  $r_c$  for pBR322 DNA (53 mol % GC). The straight line drawn in Figure 5 represents the linear equation for the balance of the total TPL-I concentration,  $c_t$  (22, 30), written in the form

$$r = r_t - \frac{1}{c_{p,t}} c_f \quad (1)$$

where  $r$  is the drug to nucleotide binding ratio,  $r_t$  is the total drug to nucleotide input ratio,  $c_f$  is the concentration of free drug, and  $c_{p,t}$  the total nucleotide concentration. According to eq 1, the straight line has the intercepts  $r = r_t$  for  $c_f = 0$  and  $c_f = c_t$  for  $r = 0$ ; the values  $(r_t; c_t)$  used in Figure 5 reflect the conditions existing at the minimum of curve 2 in Figure 6A. The ordinate of the point of intersection of the binding isotherm with this straight line (Figure 5) yields the desired critical drug to nucleotide binding ratio,  $r_c$ , for TPL-I (Table 2). Analogously, a recently published DNA binding isotherm for ethidium (22) was used to obtain the  $r_c$  value valid for the minimum of curve 1 (Figure 6A).

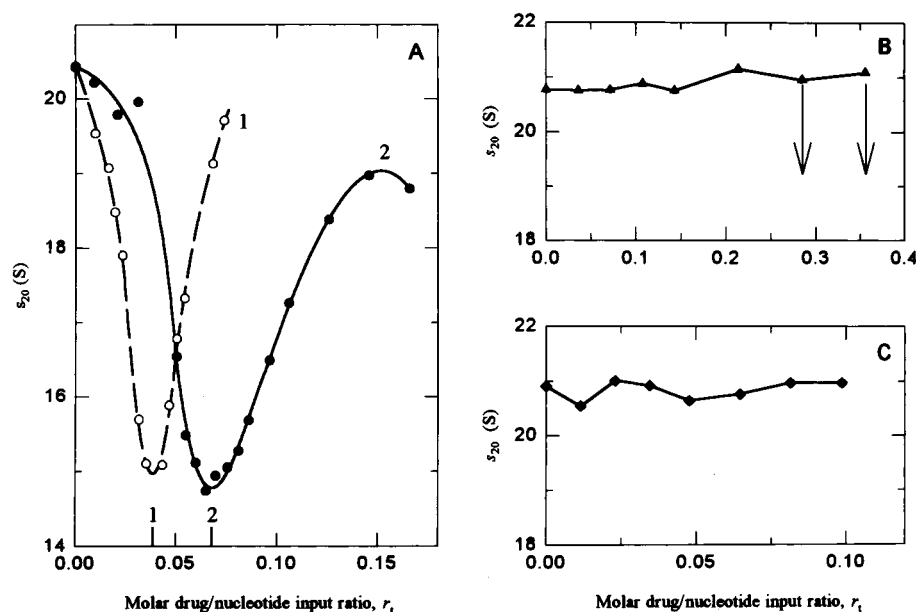


FIGURE 6: Effect of TPL-I (A, curve 2), TPL-II (B), and TPL (C) on the sedimentation behavior of supercoiled plasmid DNA from pBR322. The corresponding curve of ethidium bromide is shown for comparison (A, curve 1). DNA preparations used in A only were identical (cf. text). Buffer, 50 mM Tris HCl, 1 mM EDTA, pH 7.8 (A, C) plus 20–25 vol % DMSO (B, cf. text). Arrows in B indicate input ratios at which partial precipitation of TPL-II was observed.

Table 2: Critical Input Ratio  $(r_c)_i$ , Critical Binding Ratio  $r_c$ , and DNA Unwinding Angles  $\phi$  of Ethidium and TPL-I

drug	$(r_c)_i$	$r_c$	$\phi$ (deg)
ethidium	0.0381	0.0364	26 <sup>a</sup>
TPL-I	0.0673	0.0527	18 <sup>b</sup>

<sup>a</sup> Cf. the compilation of  $\phi$  values in Table VIII of Bauer (32).

<sup>b</sup> Calculated with the assumption  $\alpha = 1$  (see eq 2 and text).

In contrast to TPL-I, TPL-II has no significant effect on the sedimentation properties of supercoiled DNA (Figure 6B). This extremely less water soluble drug was solved in pure DMSO and stepwise added to a buffered pBR322 solution containing 20 vol % of DMSO, with the result that the DMSO content of the DNA solution increased from 20 to about 25 vol % during the titration procedure. The sedimentation coefficients were corrected for the DMSO-induced change in the viscosity and density of the buffer solution but not for a possible change in the partial specific volume of DNA. It seems conceivable that part of the water forming the immobilized hydration shell of the DNA molecule is substituted by DMSO which has a higher density compared to that of water, thus leading to a somewhat lower partial specific volume of the DNA. This would explain the small increase of the sedimentation coefficient seen in Figure 6B. Indeed, during titration of naked pGRB1 plasmid with DMSO we have observed a similar small increase in  $s_{20}$  of DNA (results not shown). On the other side, this explanation rules out any influence of TPL-II on the  $s_{20}$  value of pBR322, meaning that Figure 6B provides no argument for significant binding of TPL-II to DNA. Figure 6C demonstrates that TPL likewise leaves the sedimentation coefficient of supercoiled DNA unaffected.

#### Effects of 2-Azaanthraquinone Derivatives on DNA Topoisomerases

To determine whether the three 2-azaanthraquinones affect the activity of topoisomerases in vitro, we investigated the

influence of TPL, TPL-I, and TPL-II on the reaction of prokaryotic and eukaryotic topoisomerases using plasmid DNA and selected fragments containing defined recognition sites of the enzymes. Results for DNA gyrase from *S. noursei* are shown in Figure 7 and Table 3. It is obvious that TPL-I significantly affects the supercoiling and the cleavage reaction of gyrase, as indicated by the inhibition curves below 10  $\mu$ M ligand concentration. In contrast to that TPL-II causes only a very weak effect; inhibitory concentrations are higher than 100  $\mu$ M, which means this ligand is practically inactive (Figure 7). In Table 3 the effects of all three 2-azaanthraquinones on the supercoiling and cleavage reaction are compared including their influence on the enzyme binding to DNA, measured in the gel retardation assay. Both the  $IC_{50}$  and  $IC_{90}$  values demonstrate that TPL-I is a potent gyrase inhibitor while both TPL and TPL-II are inactive compounds. It also indicated that the gyrase–DNA interaction is very little affected by TPL-I (Table 3;  $IC_{50} \sim 150 \mu$ M), suggesting that the enzyme may interact with the substrate ligand complex but that the cleavage reaction is inhibited. As shown in Table 3, TPL-I likewise inhibits the relaxation activity of mammalian topoisomerases I and II, indicated by low  $IC_{50}$  values, while TPL and TPL-II cause only a very weak or no inhibitory effect. To get information for the drug effects on distinct cleavage sites of topoisomerases we used a restriction fragment from the plasmid pUCNC15 containing strong cleavage sites located in different sequence regions. The results shown in Figure 8 demonstrate that the two cleavage sites of topoisomerase I are affected differently by increasing TPL-I concentration. Site 1 becomes inhibited at 1  $\mu$ M and is totally blocked from the enzyme-mediated cleavage at drug concentrations higher than 5  $\mu$ M (Figure 8, arrow 1). In contrast to that, site 2 is nearly unaffected by the drug and shows a slight weakening of the cleavage activity at 50  $\mu$ M TPL-I, suggesting only that the inhibitory potency of this drug for a single site

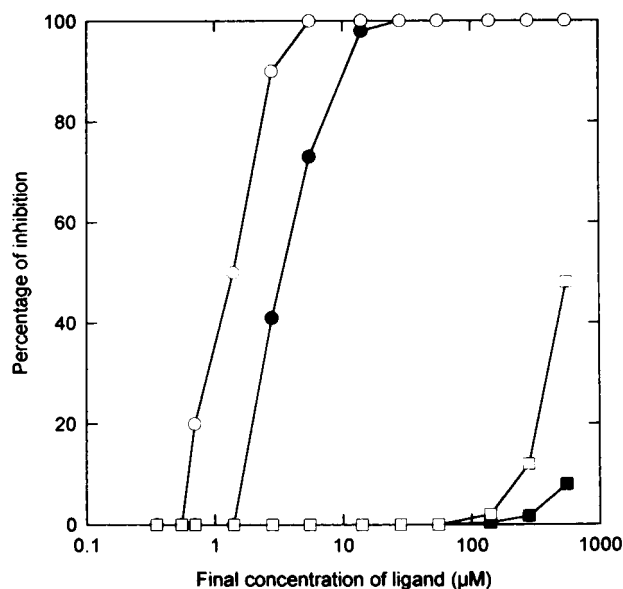


FIGURE 7: Influence of TPL-I and TPL-II on gyrase activity measured by supercoiling assay with pBR322 DNA and the cleavage reaction using a 162 bp fragment from pBR322 containing a single gyrase site. (○) Supercoiling/TPL-I; (●) cleavage/TPL-I; (□) supercoiling/TPL-II; (■) cleavage/TPL II. The gyrase cleavage site with several neighboring base pairs upstream and downstream has the sequence shown below.

↓  
 ACGCGAGGCTGGATGGCCTTCCCCATTATGAT  
 TCGGCTCCGACCTACCGGAAGGGTAATACTA  
 ↑

Table 3: Effect of 2-Azaanthraquinone Derivatives on the Activity of Topoisomerases<sup>a</sup>

ligand	Topo I		Topo II		gyrase				DNA binding	
	relaxation		relaxation		supercoiling	cleavage				
	IC <sub>50</sub>	IC <sub>90</sub>	IC <sub>50</sub>	IC <sub>90</sub>	IC <sub>50</sub>	IC <sub>90</sub>	IC <sub>50</sub>	IC <sub>90</sub>	IC <sub>50</sub>	IC <sub>90</sub>
TPL	50	80	150	300	320	n.d. <sup>b</sup>	n.d.	n.d.	650	400
TPL-I	3	9	3	9	1.3	3	3	10	150	n.d.
TPL-II	200	~400	~400	n.d.	600	n.d.	n.d.	n.d.	n.d.	n.d.

<sup>a</sup> IC<sub>50</sub> and IC<sub>90</sub> mean 50% and 90% inhibition concentration of the ligand in μM, respectively. Topoisomerases I and II were from calf thymus, gyrase was from *S. noursei*, and assays are as described under Experimental Procedures. <sup>b</sup> n.d., not detectable, which means no inactivation.

depends on the sequences around this site. Very similar results were obtained in experiments with mammalian topoisomerase II in the presence of VM 26 using the same restriction fragment (data not shown).

Filter retention assay has been used to investigate whether TPL-I can compete with mammalian topoisomerases and displace the enzymes from the *EcoRI*–*PvuII* fragment. Using the 5′-end-labeled fragment in the presence of mammalian topoisomerase I and II the enzyme–DNA complexes are trapped on the filter while the free fragment passes through it. The amount of radioactive DNA retained on the filter by bound enzymes (100% in Figure 9) decreased to about 75% and 80%, respectively, after preincubation of the fragment with increasing drug concentration. These data reflect that the affinity of both mammalian topoisomerases to this DNA fragment is diminished by TPL-I only partially.

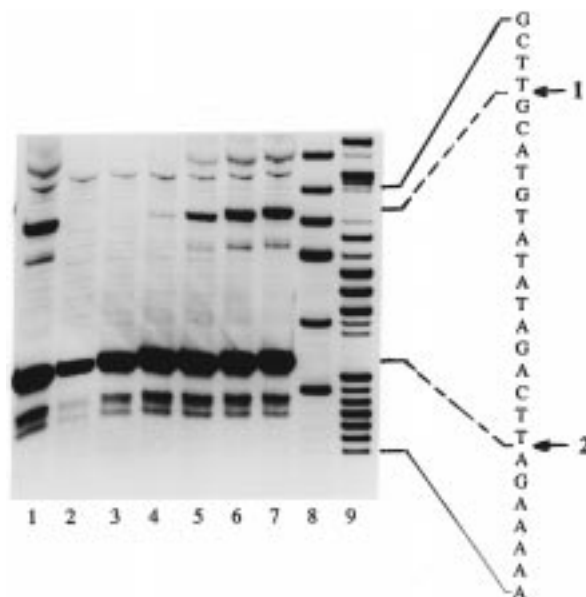


FIGURE 8: Influence of TPL-I on the cleavage sites of topoisomerase II located in a DNA fragment from pUCNC15. The gel electrophoretic analysis is shown for the sequence containing two prominent recognition sites of the enzyme, cleavage sites 1 and 2. Lanes 2–7: 50, 10, 5, 1, 0.1, 0.05 μM TPL-I; lane 1, without ligand; lane 8, G ladder; lane 9, G + A ladder. For conditions see Experimental Procedures.

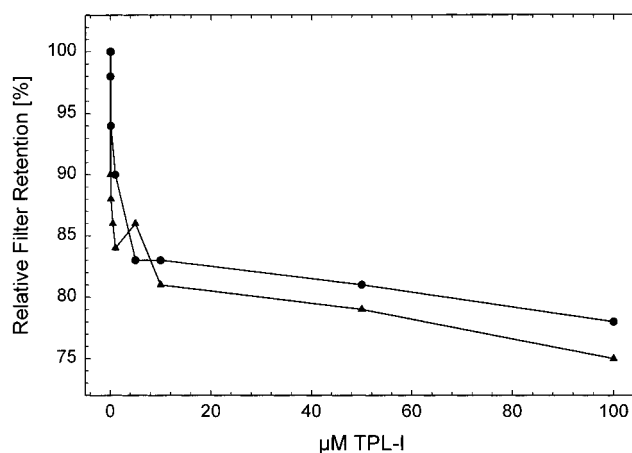


FIGURE 9: Influence of TPL-I on the filter binding of the topoisomerase I and topoisomerase II complex with the DNA fragment NC14. The amount of radioactive DNA retained on the filters in the absence of TPL-I was taken as 100%. (▲) Topo I; (●) topo II.

Gel retardation experiments also showed no pronounced displacement of the enzymes by TPL-I from their DNA complexes (data not shown).

## DISCUSSION

Modified compounds of the anthracene-9,10-dione structure with a 2-aza-ring comparable to mitoxantrone were shown to possess antitumor activity, but their affinity to nucleic acids is less characterized (5). The results presented here demonstrate the binding to DNA of a 2-azaanthraquinone related to topocladin (TPL) hitherto not reported. The analogue of TPL bearing a (dimethylamino)-ethylamino side chain (TPL-I) was shown to bind only by intercalation with a high preference to alternating purine–pyrimidine sequences in duplex DNA as judged from CD



and sedimentation measurements (Figures 3 and 6). In contrast, almost no comparable binding to DNA has been found for the parent compounds TPL and TPL-II. TPL-I only exhibited a significant increase in the  $T_m$  value (Table 1) in agreement with the highest binding constant observed for alternating purine–pyrimidine duplex DNA such as poly(dA–dT)•poly(dA–dT) with  $K_a$  value of  $\sim 6.2 \times 10^5 \text{ M}^{-1}$  (Table 1). Therefore the intercalative binding of the TPL–chromophore requires a lengthened and positively charged side chain, which is guiding the ligand to the DNA duplex structure. The data collected in Table 2 show that the  $r_c$  values for ethidium and TPL-I differ considerably from each other. This observation may be discussed on the basis of the eq 2 (31)

$$\alpha r_c \phi = \alpha' r'_c \phi' \quad (2)$$

where  $\alpha'$  and  $\alpha$  are the respective fractions of the reference drug ethidium and of TPL-I which are bound in such a way as to induce unwinding of the DNA duplex and  $\phi'$  and  $\phi$  are the unwinding angles per bound ethidium and TPL-I molecule, respectively. The consensus value for the unwinding angle of ethidium amounts to  $\phi' = 26^\circ$  (32). Under our experimental conditions, indications to another binding mode of ethidium differing from intercalation were spectroscopically not detectable (22); the free EB concentrations of about  $1 \times 10^{-7} \text{ mol/L}$  prevailing at the minimum of curve 1 (Figure 6A) are too low for a significant outside binding of ethidium. Therefore,  $\alpha'$  should be 1. With the assumption that the unwinding of DNA by TPL-I is likewise due to a single mode of interaction of the drug with DNA (i.e.,  $\alpha = 1$ ), we arrive at a value of about  $18^\circ$  for the DNA unwinding angle of TPL-I (Table 2), which is comparable to that known for nogalamycin or proflavine (33). TPL-I intercalation preferentially occurs most probably in alternating purine–pyrimidine sequences, as evidenced by the higher affinity of TPL-I for poly(dA–dT)•poly(dA–dT) and poly(dG–dC)•poly(dG–dC) than for poly(dA)•poly(dT) (Figures 2 and 3).

The structure-dependent DNA binding ability of TPL-I, TPL, and TPL-II is clearly reflected in their potency to inhibit the activity of topoisomerases. While TPL and TPL-II are nearly ineffective, TPL-I affects all three types of topoisomerases investigated. DNA supercoiling mediated by DNA gyrase and the relaxation reaction of mammalian topoisomerases I and II were efficiently inhibited by TPL-I as indicated by the  $IC_{50}$  and  $IC_{90}$  values (Table 3). These values may represent the overall effect on different recognition sites of topoisomerases contained in pBR322 DNA. To obtain more insight into the enzyme-mediated reaction at the molecular level, fragments with distinct cleavage sites of known sequence (see legend of Figure 8) were used as substrates. Obviously, binding of gyrase to the 162 bp fragment containing a single cleavage site is not essentially influenced by TPL-I whereas the cleavage reaction on a single site is clearly inhibited by this ligand (Figure 7 and Table 3). It appeared that gyrase can bind to the preformed DNA–TPL-I complex, but the enzyme is prevented from cleaving the DNA fragment. This may be explained by interaction of TPL-I with several short alternating purine–pyrimidine sequences surrounding the cleavage region, which in turn affects the double-strand breakage but not the affinity of the enzyme to the 162 bp fragment. In agreement with

this interpretation cleavage sites of mammalian topoisomerase I located in discrete regions are influenced by TPL-I differently in a sequence-dependent manner. As shown in Figure 8, TPL-I inhibits site 1 of topoisomerase I, located near the alternating purine–pyrimidine sequences that represent potential intercalative binding regions of this ligand and hence it disturbs cleavage reaction. Different from this cleavage, site 2 is not influenced under comparable conditions, which we can ascribe to the AT-containing homooligonucleotide sequence (15) flanking this site.

Since the affinity of TPL-I to poly(dA)•poly(dT) is significantly lower than to the alternating purine–pyrimidine structure the enzyme can release the weakly bound ligand from DNA. Thus, the inhibitory potency of TPL-I on topoisomerase activity we may correlate to the preferred intercalative binding of this ligand in alternating purine–pyrimidine sequences as underlined by our biophysical results.

To summarize, this investigation demonstrated the sequence-preferred binding of TPL-I which occurs by means of intercalation and suggests the usefulness of this type of ligand as a potential inhibitor of topoisomerase in vitro. A structure–activity relationship with respect to the DNA binding ability and anti-topoisomerase activity is clearly indicated by the results. Studies with these types of drugs bearing new side chains of different structure may be useful in providing new drug combinations.

## ACKNOWLEDGMENT

We thank Dr. Holger Schütz for his help in calculating binding parameters, Prof. Udo Gräfe for his permanent support of this work, and Mr. Horst Bär, Mrs. Christel Radtke, and Mrs. Sigrid Reichardt for skillful technical assistance.

## REFERENCES

- Gräfe, U., Ihn, W., Tresselt, D., Miosga, N., Kaden, U., Schlegel, B., Bormann, E.-J., Sedmera, P., and Novak, J. (1990) *Biol. Met.* 3, 39–44.
- Faulds, D., Balfour, J. A., Chrisp, P., and Langtry, H. D. (1991) *Drugs* 41, 400–449.
- Denny, W. A. (1989) *Anti-Cancer Drug Des.* 4, 241–263.
- Denny, W. A., and Wakelin, L. P. G. (1990) *Anti-Cancer Drug Des.* 5, 189–200.
- Krapcho, A. P., Petry, M. E., Getahun, Z., Landi, J. J., Stallman, J., Polsenberg, J. F., Gallagher, C. E., Maresch, M. J. and Hacker, M. P. (1994) *J. Med. Chem.* 37, 828–837.
- Lown, J. W. (1988) *Anti-Cancer Drug Des.* 3, 25–40.
- Kotovych, G., Lown, J. W., and Tong, J. P. K. (1986) *J. Biomol. Struct. Dyn.* 4, 111–125.
- Drlica, K., and Franco, R. J. (1988) *Biochemistry* 27, 2253–2259.
- Hertzberg, R. P., Caranfa, M. J., and Hecht, S. M. (1989) *Biochemistry* 28, 4629–4638.
- D'Arpa, P., and Liu, L. F. (1989) *Biochim. Biophys. Acta* 989, 163–177.
- Reece, R. J., and Maxwell, A. (1991) *Crit. Rev. Biochem. Mol. Biol.* 26 (3/4), 335–375.
- Maxwell, A. (1992) *J. Antimicrobial Chemother.* 30, 409–416.
- Capranico, G., De Isabella, P., Tinelli, S., Bigioni, M., and Zunino, F. (1993) *Biochemistry* 32, 3028–3946.
- Luck, G., Störl, J., Baguley, B., and Zimmer, Ch. (1992) *J. Biomol. Struct. Dyn.* 10, 551–564.
- Mortensen, U. H., Strevnsner, T., Krogh, S., Olesen, K., Westergaard, O., and Bonven, B. J. (1990) *Nucleic Acids Res.* 18, 1983–1989.
- Hajduk, S. L., Klein, V. A., and Englund, P. T. (1984) *Cell* 36, 483–492.

17. Simon, H., Roth, M., and Zimmer, Ch. (1995) *FEBS Lett.* 373, 88–92.
18. Strausfeld, U., and Richter, A. (1989) *Prep. Biochem.* 19, 37–48.
19. Marini, J. C., Miller, K. G., and Englund, P. T. (1980) *J. Biol. Chem.* 255, 4976–4979.
20. Simon, H., Wittig, B., and Zimmer, Ch. (1994) *FEBS Lett.* 353, 79–83.
21. Störl, K., Störl, J., Zimmer, Ch. and Lown, J. W. (1993) *FEBS Lett.* 317, 157–162.
22. Triebel, H. Bär, H., Walter, A., Burckhardt, G. and Zimmer, Ch. (1994) *J. Biomol. Struct. Dyn.* 11, 1085–1105.
23. Triebel, H., Bär, H., Geuther, R., and Burckhardt, G. (1995) *Prog. Colloid Polym. Sci.* 99, 45–54.
24. Fritzsche, H., and Walter, A. (1989) in *Chemistry and Physics of DNA–Ligand Interactions* (Kallenbach, N. R., Ed.) pp 1–35, Adenine Press, Schenectady, NY.
25. Zimmer, Ch., and Luck, G. (1992) in *Advances in DNA Sequence Specific Agents* (Hurley, H., Ed.) Vol. 1, 51–88, JAI Press Inc., Greenwich, CT.
26. Bradley, D. F., and Lifson, S. (1968) in *Molecular Association in Biology* (Pullman, B., Ed.) pp 261–270, Academic Press Inc., New York.
27. McGhee, G. D., and von Hippel, P. H. (1974) *J. Mol. Biol.* 86, 469–489.
28. Waring, M. In *Progress in Molecular and Subcellular Biology* (Hahn, F. E., Ed.) Vol. 2, pp 216–231, Springer-Verlag, Berlin.
29. Bauer, W., and Vinograd, J. (1971) In *Progress in Molecular and Subcellular Biology* (Hahn, F. F., Ed.) Vol. 2, pp 181–215, Springer-Verlag, Berlin.
30. Stutter, E., Schütz, H., and Berg, H. (1988) in *Bioactive Molecules* Vol. 6, Anthracycline and Anthracenedione–based Anticancer Agents (Lown, J. W., Ed.) pp 254–293, Elsevier Science Publishers, Amsterdam.
31. Dougherty, G., and Waring, M. J. (1982) *Biophys. Chem.* 15, 27–40.
32. Bauer, W. (1990) In *Landoldt-Börnstein New Series, Group VII, Vol. 1, Nucleic Acids, Subvolume d, Physical Data II*, pp 1–30, Springer-Verlag, Berlin.
33. Waring, M. (1981) *Annu. Rev. Biochem.* 50, 159–192.

BI9724220